Vietnam Journal of Mechanics, VAST, Vol. 30, No. 1 (2008), pp. 20 – 32

POTENTIAL EVAPOTRANSPIRATION ESTIMATION AND ITS EFFECT ON HYDROLOGICAL MODEL RESPONSE

Vu Van Nghi[1]
State Key Laboratory of Hydrology,
Water Resources and Hydraulic Engineering,
Hohai University, no. 1 Xikang Road, Nanjing 210098, China
Do Duc Dung, Dang Thanh Lam
Southern Institute for Water Resources Planning,
271/3 An Duong Vuong Street, District 5,
Ho Chi Minh City, Vietnam

Abstract. Potential evapotranspiration can be directly calculated by the Penman-Monteith equation, known as the one-step method. The approach requires data on the land cover and related-vegetation parameters based on AVHRR and LDAS information, which are available in recent years. The Nong Son basin, a sub-catchment of the Vu Gia-Thu Bon basin in the Central Vietnam, is selected for this study. To this end, NAM model was used; the results obtained show that the NAM model has the potential to reproduce the effects of potential evapotranspiration on hydrological response. This is seemingly manifested in the good agreement between model simulation of discharge and the observed at the stream gauge.
Keywords: Potential evapotranspiration, Penman-Monteith method, Piche evaporation, Leaf area index (LAI), Normalized difference vegetation index (NDVI)

1. INTRODUCTION

One of the key inputs to hydrological modeling is potential evapotranspiration, which refers to maximum meteorologically evaporative power on land surface. Two kinds of potential evapotranspiration are necessary to be defined: either from the interception or from the root zone when the interception is exhausted but soil water is freely available, specifically at field capacity (see [10], [32]). The actual evapotranspiration is distinguished from the potential through the limitations imposed by the water deficit. Evapotranspiration can be directly measured by lysimeters or eddy correlation method but expensively and practically only in research over a plot for a short time. The pan or Piche evaporation has long records with dense measurement sites. To apply it in hydrological models, however, first, a pan/Piche coefficient, K_p, then a crop coefficient, K_c, must be multiplied as well. Due to the difference on sitting and weather conditions, K_p is often expressed as a function of local environmental variables such as wind speed, humidity, upwind fetch, etc. A global equation of K_p is still lack. The values of K_c from the literature are empirical, most for agricultural crops, and subjectively selected. Moreover, the observed Piche data show

[1]Corresponding author:
Email: vuvannghi@yahoo.com Tel: 0086.15850569677

some erroneous results which are difficult to explain (see [22]), and the pan evaporameter is not considered accurate (see [7], [8]). On the other hand, a great number of evaporation models has been developed and validated, from the single climatic variable driven equations (see [29]) to the energy balance and aerodynamic principle combination methods (see [23]). Among them, probably the Penman equation is the most physically sound and rigorous. Monteith (see [19]) generalized the Penman equation for water-stressed crops by introducing a canopy resistance. Now the Penman–Monteith model is widely employed.

As a result, in this study the Penman-Monteith method is selected to compute directly potential evapotranspiration according to the vegetation dataset at 30s resolution based on AVHRR (Advanced Very High Resolution Radiometer) and LDAS (Land Data Assimilation System) information for the Nong Son catchment. To assess the suitability of this approach, the conceptual rainfall-runoff model known as NAM (see [9]) is used to examine its effect on hydrological response.

2. POTENTIAL EVAPOTRANSPIRATION MODEL DESCRIPTION

2.1. Penman-Monteith equation

Potential evapotranspiration can be calculated directly with the Penman-Monteith equation (see [3]) as follows:

$$\lambda ET = \frac{\Delta(R_n - G) + \rho_a c_p \dfrac{\left(e_s - e_a\right)}{r_a}}{\Delta + \gamma\left(1 + \dfrac{r_s}{r_a}\right)}, \tag{1}$$

where ET is the evapotranspiration rate (mm.d^{-1}); λ is the latent heat of vaporization (= 2.45 MJ.kg^{-1}); R_n is the net radiation; G is the soil heat flux (normally with a relatively small value, in general, it may be ignored (see [3])); e_s is the saturated vapor pressure; e_a is the actual vapor pressure; $(e_s - e_a)$ represents the vapour pressure deficit of the air; ρ_a is the mean air density at constant pressure; c_p is the specific heat of the air (=1.01 kJ.kg^{-1}K^{-1}); Δ represents the slope of the saturation vapour pressure temperature relationship; γ is the psychrometric constant; and r_s and r_a are the (bulk) surface and aerodynamic resistances.

The Penman-Monteith approach as formulated above includes all parameters that govern energy exchange and corresponding latent heat flux (evapotranspiration) from uniform expanses of vegetation. Most of the parameters are measured or can be readily calculated from weather data. The equation can be utilized for the direct calculation of any crop evapotranspiration as the surface and aerodynamic resistances are crop specific.

2.2. Factors and parameters determining ET

2.2.1. *Land surface resistance parameterization*

a. Aerodynamic resistance

The rate of water vapor transfer away from the ground by atmospheric turbulent diffusion is controlled by aerodynamic resistance r_a (s.m^{-1}), which is inversely proportional to wind speed and changes with the height of the vegetation covering the ground, as

$$r_a = \frac{\ln\left[\left(z_u - d\right)/z_{om}\right] \ln\left[\left(z_e - d\right)/z_{oh}\right]}{\kappa^2 u_z}, \tag{2}$$

where z_u is the height of wind measurements (m); z_e is the height of humidity measurements (m); d is the zero plane displacement height (m); z_{om} is the roughness length governing momentum transfer (m); z_{oh} is the roughness length governing transfer of heat and vapour (m); u_z is the wind speed; and κ is the von-Karman constant (= 0.41).

Many studies have explored the nature of the wind regime in plant canopies. d and z_{om} have to be considered when the surface is covered by vegetation. The factors depend upon the crop height and architecture. Several empirical equations (see [5], [11], [20], [31]) for the estimate of d, z_{om} and z_{oh} have been developed. In this study, estimate can be made of r_a by assuming (see [4]) that $z_{om} = 0.123\ h_c$ and $z_{oh} = 0.0123\ h_c$, and (see [20]) that $d = 0.67\ h_c$, where h_c (m) is the mean height of the crop.

b. Surface resistance

The 'bulk' surface resistance r_s (s.m^{-1}) describes the resistance of vapour flow through the transpiring crop and evaporating soil surface. Where the vegetation doesn't completely cover the soil, the resistance factor should indeed include the effects of the evaporation from the soil surface. If the crop isn't transpiring at a potential rate, the resistance depends also on the water status of the vegetation. An acceptable approximation (see [1], [3]) to a much more complex relation of the surface resistance of fully dense cover vegetation is:

$$r_s = \frac{r_l}{LAI_{\text{active}}}, \tag{3}$$

where r_l is the bulk stomatal resistance of the well-illuminated (s.m^{-1}); and LAI_{active} is the active (sunlit) leaf area index (m^2 leaf area over m^2 soil surface).

A general equation (see [2], [15], [30]) for LAI_{active} is:

$$LAI_{active} = 0.5LAI. \tag{4}$$

The bulk stomatal resistance, r_l, is the average resistance of an individual leaf. This resistance is crop specific and differs among crop varieties and crop management. It usually increases as the crop ages and begins to ripen. There is, however, a lack of consolidated information on changes in r_l over time for the different crops. The information available in the literature on stomatal resistance is often oriented toward physiological or ecophysiological studies. The stomatal resistance is influenced by climate and by water availability. However, the influences vary from one crop to another and different varieties can be affected differently. The resistance increases when the crop is water stressed and the soil water availability limits crop evapotranspiration. Some studies (see [13], [14], [18], [26], [33]) indicate that stomatal resistance is influenced to some extent by radiation intensity, temperature and vapour pressure deficit.

If the crop is amply supplied with water, the crop resistance, r_s, reaches a minimum value, known as the *basis canopy resistance*. The transpiration of the crop is then maximum and referred to as potential transpiration. The relation between r_s and the pressure head in the root zone is crop dependent. Minimum values of r_s range from 30 s.m^{-1} for arable crops to 150 s.m^{-1} for forest. For grass a value of 70 s.m^{-1} is often used (see [7]). It should be noted that r_s cannot be measured directly, but has to be derived from the Penman-Monteith formula where ET is obtained from e.g. the water balance of a lysimeter.

The Leaf Area Index (LAI), a dimensionless quantity, is the leaf area (upper side only) per unit area of soil below it. The active LAI is the index of the leaf area that actively contributes to the surface heat and vapour transfer. It is generally the upper, sunlit portion of a dense canopy. The LAI values for various crops differ widely but values of 3-5 are

common for many mature crops. For a given crop, the green LAI changes throughout the season and normally reaches its maximum before or at flowering. LAI further depends on the plant density and the crop variety. Several studied and empirical equations (see [18], [31]) for the estimate of LAI have been developed. If h_c is the mean height of the crop, then the LAI can be estimated (see [1]) by:

$$\begin{array}{ll} LAI = 24h_c & \text{(clipped grass with } 0.05 < h_c < 0.15\,m\text{)} \\ LAI = 5.5 + 1.5\ln(h_c) & \text{(alfalfa with } 0.10 < h_c < 0.50\,m\text{)} \end{array} . \tag{5}$$

As an alternative, spectral vegetation indices from satellite-based spectral observations, such as $NDVI$ (normalized difference vegetation index), or simple ratio ($SR = (1 + NDVI)/(1 - NDVI)$); are widely used to extract vegetation biophysical parameters of which LAI is the most important. The use of monthly vegetation index is a good way to take into account the phenological development of the LAI, as well as the effects of prolonged water stresses that reduce the LAI (see [17]). In this study, monthly maximum composite 1-km resolution $NDVI$ dataset obtained from NOAA-AVHRR (National Oceanic and Atmospheric Administration-Advanced very High Resolution Radiometer) in 1992, 1995 and 1996 were used to estimate LAI. The simple relationships between LAI and $NDVI$ were taken from SiB2 (see [25]). For evenly distributed vegetation, such as grass and crops:

$$LAI = LAI_{\max}\frac{\ln(1 - FPAR)}{\ln(1 - FPAR_{\max})}. \tag{6}$$

For clustered vegetation, such as coniferous trees and shrubs:

$$LAI = \frac{LAI_{\max}FPAR}{FPAR_{\max}}, \tag{7}$$

where $FPAR$ is the fraction of photosynthetically active radiation absorbed by the canopy, calculated as:

$$FPAR = \frac{(SR - SR_{\min})(FPAR_{\max} - FPAR_{\min})}{SR_{\max} - SR_{\min}}, \tag{8}$$

where $FPAR_{max}$ and $FPAR_{min}$ are taken as 0.950 and 0.001, respectively. SR_{max} and SR_{min} are SR values corresponding to 98 and 5% of $NDVI$ population, respectively.

Land cover classes of needleleaf deciduous, evergreen and shrub land thicket are treated as clumped vegetation types (see [24]). In cases where there is a combination of clustered and evenly distributed vegetation, LAI can be calculated by a combination of Equation (6) and (7):

$$LAI = (1 - F_{cl})LAI_{\max}\frac{\ln(1 - FPAR)}{\ln(1 - FPAR_{\max})} + F_{cl}\frac{LAI_{\max}FPAR}{FPAR_{\max}}, \tag{9}$$

where F_{cl} is the fraction of clumped vegetation in the area.

2.2.2. *Surface exchanges*

a. Saturated vapor content of air

The saturated vapor pressure is related to temperature; if e_s is in kilopascals (kPa) and T is in degrees Celsius (°C), an approximate equation (see [28]) is:

$$e_s = 0.6108\exp\left(\frac{17.27T}{237.3 + T}\right). \tag{10}$$

It is important in building physically based models of evaporation that not only is e_s a known function of temperature, but also so is Δ (kPa.C^{-1}), the gradient of this function, de_s/dT. This gradient is given by:

$$\Delta = \frac{4098 e_s}{(237.3 + T)^2}. \tag{11}$$

The relative humidity (RH %) expresses the degree of saturation of the air as a ratio of the actual (e_a) to the saturation (e_s) vapour pressure at the same temperature (T):

$$RH = 100 \frac{e_a}{e_s}. \tag{12}$$

b. Sensible heat

The density of (moist) air can be calculated from the ideal gas laws, but it is adequately estimated from:

$$\rho_a = 3.486 \frac{P}{275 + T}, \tag{13}$$

where P is the atmospheric pressure in kPa. Assuming 20°C for a standard atmosphere, P as a function of height z (in meters) above the mean sea level can be employed to calculate by:

$$P = 101.3 \times \left(\frac{293 - 0.0065 z}{293} \right)^{5.26}. \tag{14}$$

c. Psychrometric constant

The psychrometric constant, γ (kPa.°C^{-1}), is given by:

$$\gamma = \frac{c_p P}{\varepsilon \lambda} = 0.665 \times 10^{-3} P, \tag{15}$$

where ε is the ratio the molecular weights of water vapor and dry air, equals to 0.622. Other parameters in the equation are defined above.

2.2.3. *Radiation balance at land surface*

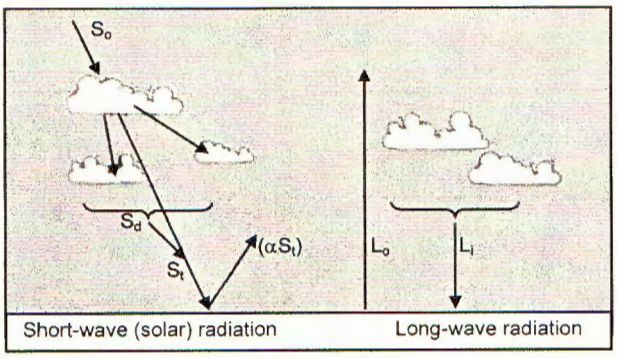

Fig. 1. Radiation balance at the earth's surface

In the absence of restrictions due to water availability at the evaporative surface, the amount of radiant energy captured at the earth's surface is the dominant control on regional evaporation rates. As a monthly average, the radiant energy at the ground may

be the most "portable" meteorological variable involved in evaporation estimation, in the sense that it is driven by astronomical rather than local climate conditions. Understanding surface radiation balance, and how to quantify it, is therefore crucial to understanding and quantifying evaporation.

a. Net short wave radiation

The net short wave radiation S_n (MJ.m^{-2}.day^{-1}) is that portion of the incident short wave radiation captured at the ground taking into account losses due to reflection, and given by:

$$S_n = S_t\,(1-\alpha)\,, \tag{16}$$

where α is the reflection coefficient or albedo; and S_t is the solar radiation (MJ.m^{-2}.day^{-1}).

The values of albedo for broad land cover classes are given in various scientific literatures. The solar radiation S_t (MJ.m^{-2}.day^{-1}) in most the cases can be estimated (see [6]) from measured sunshine hours according to the following empirical relationship:

$$S_t = \left(a_s + b_s\frac{n}{N}\right) S_0\cdot, \tag{17}$$

where S_0 is the extraterrestrial radiation (MJ.m^{-2}.day^{-1}); a_s is the fraction of S_0 on overcast days ($n = 0$); $(a_s + b_s)$ is the fraction of S_0 on clear days (for average climates$a_s = 0.25$ and$b_s = 0.50$); n is the bright sunshine hours per day (h); N is the total day length (h); and n/N is the cloudiness fraction. Valuesfor N and S_0 for different latitudes are given and tabulated in various handbooks (see [3], [7]).

b. Net long wave radiation

The exchange of long wave radiation L_n (MJ.m^{-2}.day^{-1}) between vegetation and soil on the one hand, and atmosphere and clouds on the other, can be represented by the following radiation law (see [3], [7], [16]):

$$L_n = \sigma\left(0.9\frac{n}{N} + 0.1\right)(0.34 - 0.14\sqrt{e_a})\,(T+273)^4\,, \tag{18}$$

where σ is the Stefan-Boltzmann constant (4.903×10^{-9} MJ.m^{-2}K^{-4}.day^{-1}).

c. Net radiation

The net radiation R_n (MJ.m^{-2}.day^{-1}) is the difference between the incoming net short wave radiation S_n and the outgoing net long wave radiation L_n:

$$R_n = S_n - L_n. \tag{19}$$

Using Equation (17) and substituting (16), (18) into (19), for general purposes when only sunshine, temperature, and humidity data are available, Equation (19) can be rewritten as follow:

$$R_n = \left(0.25 + 0.5\frac{n}{N}\right) S_0 - \left(0.9\frac{n}{N} + 0.1\right)(0.34 - 0.14\sqrt{e_a})\,(T+273)^4\,\sigma. \tag{20}$$

3. STUDY AREA AND DATA PROCESSING

3.1. Study area description

The study area (14°41'-15°45'N and 107°40'-108°20'E) covers 3,160 km^2 with the gauging station at Nong Son. It is a mountainous sub-basin of the Vu Gia-Thu Bon basin located in the East of Truong Son mountain range, the center of Vietnam (Fig. 2). The altitude ranges from several meters to 2,550 meters above sea level (data derived from DEM 90×90). The mean slope and the river network density of the basin are 24.2% and

0.41 km/km^2 respectively. The main soil in the basin is granite, alluvial soil, i.e. iron pan, grandiosity, deposit alluvia, clay and sand.

In this study area, there are only four rain gauges in which only one gauge collects hourly data, one climatic station at Tra My, and one discharge gauge at Nong Son. In general, hydro-meteorological station network is poor, i.e. a rain gauge is installed every 800 km^2. The data have been provided by the Hydro-Meteorological Data Center (HMDC), the Ministry of Natural Resources and Environment (MONRE) of Vietnam.

Due to the effects of predominating wind direction (North-East in the rainy season) and topography, rainfall in the basin is very high and significantly varies in space and time. According to the rainfall records from 1980 to 2004, the rainfall distribution spatially increases from East to West and from North to South (the mean annual rainfall at Tra My is more than 4,000 mm whereas at Thanh My just more than 2,200 mm).

Fig. 2. Nong Son Catchment

For seasonal rainfall distribution, the rainfall in October and November reaches up to 1,800 mm. The period of the North-East wind lasts from September to December coinciding with the rainy season on the basins. Although the rainy season only lasts just for 4 mouths, the rainfall amount occupies 70% of the annual rainfall. Furthermore, the annual rainfall amounts also show yearly variations from 2,417 mm (1982) to 6,259 mm (1996) with an average value of 3,697 mm. The annual runoff coefficient (runoff/precipitation) in this period varies intensively between 0.49 (1982) and 0.81 (1995) with an average value of 0.73.

3.2. Land cover data and vegetation-related parameters

The land cover data was obtained from UMD 1km Global Land Cover (http://www.geog.umd.edu/landcover/1km-map.html) based on AVHRR and LDAS (Land Data Assimilation System) information. AVHRR provides information on globe land classification at 30 s resolution (see [12]). In this study area, there are ten categories of land cover in which evergreen broadleaf occupies a largest area of 48.7% in total, followed by

deciduous needleleaf 19.3%, wooded grasslands 18.0%, deciduous broadleaf 4.2%, woodland 3.3%, mixed cover 3.2%, closed shrublands 2.0%, open shrublands 0.6%, grasslands 0.4%, and crop land 0.2%.

For each type of vegetation in the Nong Son catchment, the vegetation parameters such as minimum stomata resistance, leaf-area index, albedo, and zeroplane displacement are derived from http://www.ce.washington.edu/pub/HYDRO/cherkaue/VIC-NL/Veg/veg_lib; these are as provided in Table 1.

Table 1. Vegetation-related parameters for each type of vegetation in the Nong Son catchment

Vegetation classification	Albedo	Minimum stoma resistance (s/m)	Leaf area index	Roughness length (m)	Zero-plane Displacement (m)
Evergreen broadleaf forest	0.12	250	3.40–4.40	1.4760	8.040
Deciduous needleleaf forest	0.18	125	1.52–5.00	1.2300	6.700
Deciduous broadleaf forest	0.18	125	1.52–5.00	1.2300	6.700
Mixed forest	0.18	125	1.52–5.00	1.2300	6.700
Woodland	0.18	125	1.52–5.00	1.2300	6.700
Wooded grasslands	0.19	135	2.20–3.85	0.4950	1.000
Closed shrublands	0.19	135	2.20–3.85	0.4950	1.000
Open shrublands	0.19	135	2.20–3.85	0.4950	1.000
Grasslands	0.20	120	2.20–3.85	0.0738	0.402
Croplands	0.10	120	0.02–5.00	0.0060	1.005

3.3. Meteorological data

In the Penman-Monteith method, meteorological data such as mean temperature, relative humidity, sunshine hour, and wind speed are required. The observed data from the Tra My climatic station for the period of 1980-2004 were used in this study.

- Air temperature (T): The research basin is located in the monsoon tropical zone. Based on the data at Tra My station, it shows an average annual temperature of 24.5°C. Average lowest temperature during December-February ranges 20 to 22°C with an absolutely minimum of 10.4°C, and average highest temperature during long period (April to September) ranges 26 to 27°C with an absolutely maximum value of 40.5°C.

- Relative humidity (RH): The study area lies in a mountainous tropical humidity zone, and as such the value of relative humidity is fairly high and stable with an average value of 87%. The observed data shows that the maximum humidity is in October to December reaching 92% while the minimum is somewhere between April and July do get as high as 83% or more.

- Sunshine hours (n): Because it lies in the high rainy sub-region, sunshine hours in the study area are relatively lower than those in the surrounding areas with a mean annual value of 5.1 hours/day. The monthly average of sunshine hours varies from 2.0 hours/day in December to 7.0 hours/day in May.

- Wind speed and direction (u): The popular directions of wind are South-East and South-West from May to September, East and North-East from October to April. The wind speed is moderate with an average annual value of 0.9 m/s.

Table 2. Monthly average meteorological characteristics in the Nong Son catchment

Characteristics	Jan	Feb	Mar	Apr	May	Jun	Jul	Aug	Sep	Oct	Nov	Dec	Ave.
T (°C)	20.6	21.9	24.0	26.2	26.9	27.1	27.1	26.9	25.9	24.4	22.6	20.6	24.5
RH (%)	89.4	87.6	84.6	82.8	84.1	83.8	83.4	84.1	87.6	90.4	92.5	92.4	86.9
n (hours/day)	3.5	4.7	5.9	6.5	6.9	6.6	6.7	6.3	5.2	3.9	2.6	2.0	5.1
u (m/s)	0.8	1.1	1.0	0.9	0.8	0.8	0.8	0.8	0.8	0.9	0.8	0.7	0.9

4. RESULTS AND DISCUSSION

From the land cover data and vegetation-related parameters in the Nong Son catchment, and the monthly meteorological data at the Tra My climate station in the period of 1980-2004, potential evapotranspiration values were determined by the Penman-Monteith model. Table 3 and Fig. 3 show the results of monthly potential evapotranspiration.

Table 3. Calculated monthly mean potential evapotranspiration for each vegetation type and average over basin in the Nong Son catchment

ET (mm)	Jan	Feb	Mar	Apr	May	Jun	Jul	Aug	Sep	Oct	Nov	Dec	Annual
Evergreen broadleaf	56	63	93	111	123	122	129	123	99	75	54	47	1,094
Deciduous needleleaf	53	56	87	124	147	142	149	141	108	84	55	47	1,195
Deciduous broadleaf	53	56	87	124	147	142	149	141	108	84	55	47	1,195
Mixed cover	53	56	87	124	147	142	149	141	108	84	55	47	1,195
Woodland	53	56	87	124	147	142	149	141	108	84	55	47	1,195
Wooded grasslands	58	68	108	131	137	130	137	128	106	83	59	49	1,194
Closed shrublands	56	66	105	129	135	127	134	126	104	81	57	48	1,170
Open shrublands	56	66	105	129	135	127	134	126	105	86	62	53	1,186
Grasslands	63	74	108	124	132	125	131	125	105	86	62	53	1,188
Crop land	20	9	32	92	123	123	134	132	101	54	22	10	853
Areal	56	62	94	119	133	129	136	129	103	79	55	48	1,144

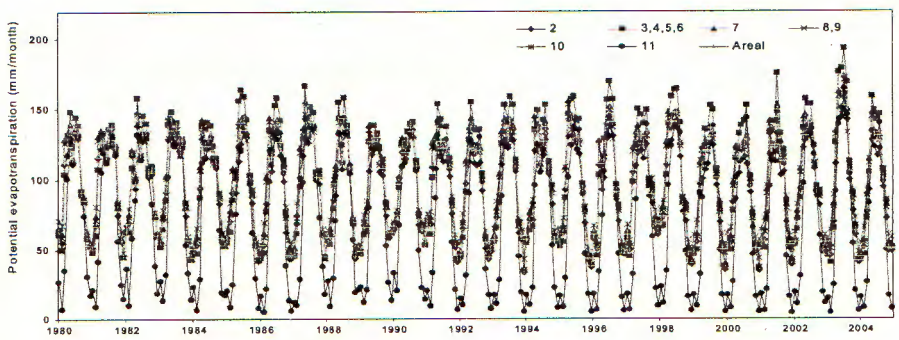

Fig. 3. Calculated m onthly potential evapotranspiration for each type of vegetation and average over basin in the Nong Son catchment in the 1980-2004 period. Note: 2- Evergreen broadleaf; 3, 4, 5, 6- Deciduous needleleaf, Deciduous broadleaf, Mixed cover, and Woodland; 7- Wooded grasslands; 8, 9- Closed shrublands, and Open shrublands; 10- Grasslands; 11- Crop land; and Areal-Average potential evapotranspiration over basin

Based on the result of Southern Institute of Water Resources Research, the potential evapotranspiration was derived from Piche tube observation values while multiplying it by correction factors, this is usually called ET_{Piche} (see [27]).

Table 4. Monthly mean potential evapotranspiration estimated by the Penman-Montheith method and Piche tube data in the Nong Sơn catchment in the 1980-2004 period

ET (mm)	Jan	Feb	Mar	Apr	May	Jun	Jul	Aug	Sep	Oct	Nov	Dec	Annual
ET_{P-M}	56	62	94	119	133	129	136	129	103	79	55	48	1,144
ET_{Piche}	68	82	118	119	133	120	128	125	103	84	62	56	1,198

The comparative performance of ET by the Penman-Monteith method (ET_{P-M}) and ET_{Piche} during the 1980-2004 period, Table 4 shows a relatively small difference in the annual value, precisely less than 5%. However there is difference in monthly distribution, particularly from January to March with $ET_{Piche} > ET_{P-M}$ of about 27%. Based on the climatic characteristics in Table 2, ET_{P-M} shows a closer accord with the seasonal distribution. Fig. 4 shows that ET_{Piche} values are somewhat unrealistic, for example, potential evaporation in June 1985 has an average value of 7 mm/day which is too high for any natural tropical humid area. This result agrees with that of Nguyen (see [22]) that the observed Piche data often give erroneous outputs.

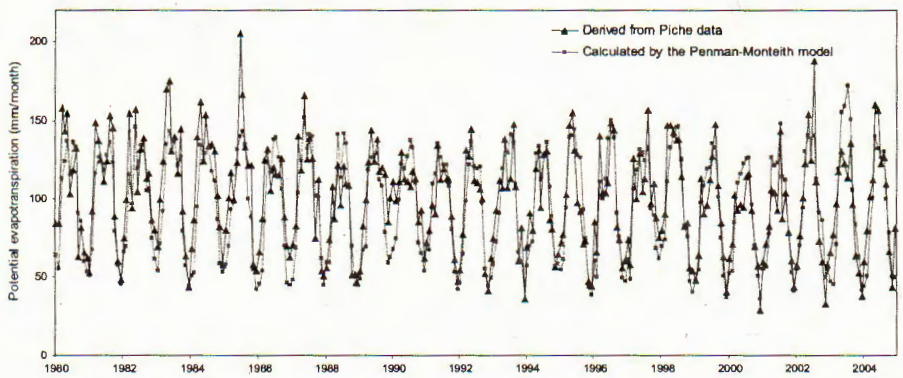

Fig. 4. Comparison of monthly potential evapotranspiration estimated by the Penman-Montheith method and Piche tube data in the 1980-2004 period

In order to assess further the suitability of the potential evapotranspiration estimated directly by the Penman-Monteith method and that derived from the Piche data, the NAM conceptual model was used to simulate the hydrology of the study area in the 1983-2003 period. The NAM model performance is evaluated with a set of two statistical criteria, Bias and Nash-Sutcliffe efficiency coefficient (see [21]).

Discharge simulated by using the input data of ET_{Piche} and ET_{P-M} is shown in Fig. 5 as monthly averages. Performance measures are given in Table 5. While the overall simulated discharge with the input of ET_{P-M} is slightly smaller than the observed, in the case of ET_{Piche} it is the reverse. However, the overall water balances (Bias) in both cases are realistic (less than 5%). The good thing here is that ET_{P-M} provides a better

Table 5. Performance measures of two potential evapotranspiration inputs ET_{P-M} and ET_{Piche} during the simulation (1983-2003) period for the Nong Son catchment

Performance statistics	ET_{P-M}	ET_{Piche}
Bias (%)	3.100	-2.636
Nash-Sutcliffe efficiency, R^2	0.880	0.802

model performance in the term of the Nash-Sutcliffe efficiency (0.880) against that of ET_{Piche}(0.802) with respect to the model simulation of the discharge at the stream gauge.

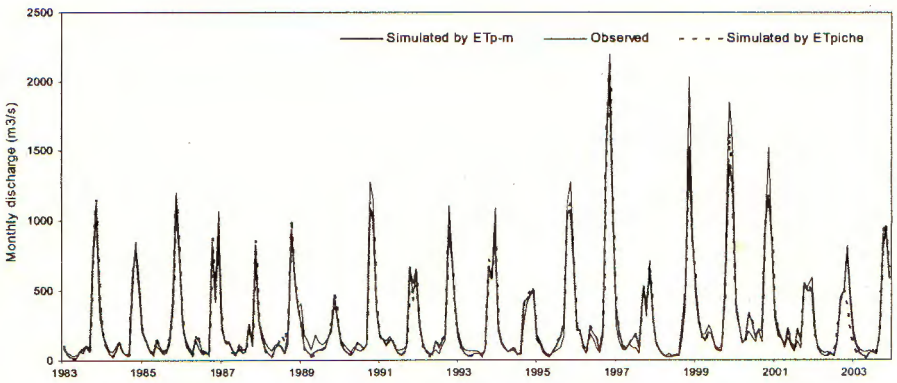

Fig. 5. Observed vs. simulated monthly discharge for the 1983-2003 period using the potential evapotranspiration inputs of ET_{Piche} and $ET_{\text{P-M}}$

5. CONCLUSION

The Penman-Monteith method was used to compute directly the potential evapotranspiration for the Nong Son catchment. The approach was assessed the suitability through the hydrological model response performance. The result of this approach shows a close agreement between the simulated and observed discharges at the stream gauge in comparison with Piche observation. The main conclusion here is that the Penman-Monteith evapotranspiration is more reliable than the Piche method as well as using pan data. Although the approach requires data on land cover and vegetation-related parameters, these data are available in websites in recent years. Hence, due to the importance of evapotranspiration in water balance, the Penman-Monteith method is recommended as the sole standard method to apply for similar catchments.

ACKNOWLEDGEMENTS

The supports of Danish Hydraulic Institute (DHI) in providing the NAM license for its application and data by Southern Institute of Water Resources are duly acknowledged. We would like to thank the anonymous reviewers and editors for their pertinent comments, leading to improvements in the paper.

REFERENCES

1. R.G. Allen, A Penman for all seasons, *Jour. of Irr. & Drainage Engineering* **112** (4) (1987) 348-368.
2. R.G. Allen, *Irrigation Engineering Principles*, Utah State University, Utah, 1995.
3. R.G. Allen, L.S. Pereira, D. Raes and M. Smith, *Crop evapotranspiration-Guidelines for computing crop water requirements – FAO Irrigation and Drainge Paper 56*, FAO, Rome, 1998.
4. W. Brutsaert, *Comments on surface roughness parameters and the height of dense vegetation, J. Meteorol. Soc. Japan* **53** (1975) 96-97.
5. W. Brutsaert, Heat and mass transfer to and from surfaces with dense vegetation or similar permeable roughness, *Boundary-Layer Meteorology* **16** (1979) 365-388.
6. W. Brutsaert, *Evaporation into the atmosphere*, D. Reidel Pub. Co., Dordrecht, Holland, 1982.
7. P.J.M. De Laat, and H.H.G. Savenije, *Principle of hydrology*, Lecture note, IHE, Deft, 2000.
8. DHI Water & Environment, *NAM calculation - DHI materials*, Horsholm, Denmark, 2003.
9. DHI Water & Environment, *MIKE 11*, Horsholm, Denmark, 2004.
10. C.A. Federer, C.J. Vorosmarty and B. Fekete, Intercomparison of methods for potential evapotranspiration in regional or global water balance models, *Water Resour. Res.* **32** (1996) 2315-2321.
11. J.R. Garrat and B.B. Hicks, *Momentum, heat and water vapour transfer to and from natural and artificial surface*, *Quarterly Journal of the Royal Meteorological Society* **99** (1973) 680-687.
12. M. Hansen, R. DeFries, J. R. G. Townshend and R. Sohlberg, *Global land cover classification at 1km resolution using a decision tree classifier*, *International J. of Remote Sensing* **21** (2000) 1331-1365.
13. P. Irannejad and Y. Shao, Description and validation of the atmosphere-land-surface interaction scheme (ALSIS) with HAPEX and Cabauw data, *Global and Planetary Change* **19** (1-4) (1998) 87-114.
14. P.G. Jarvis, The interpretation of the variation in leaf water potential and stomatal conductance found in canopies in the field, *Philosophical Transactions of the Royal Society of London Series B* **273** (1976) 593-610.
15. H. Kirnak and T. H. Short, An Evapotranspiration Model for Nursery Plants Grown in a Lysimeter Under Field Conditions, *Turk J Agric For* **25** (2001) 57-63.
16. D.R. Maidment, *Handbook of hydrology*, MacGraw-Hill, New York, 1993.
17. P. Maisongrande, A. Ruimy, G. Dedieu and B. Saugier, *Monitoring seasonal and interannual variations of gross primary productivity and net ecosystem productivity using a diagnostic model and remotely-sensed data*, Tellus, 47B, 1985, pp. 178-190.
18. X. Mo, S. Liu, Z. Lin and W. Zhao, Simulating temporal and spatial variation of evapotranspiration over the Lushi basin, *Journal of Hydrology* **285** (2004) 125-142.
19. J.L. Monteith, *Evaporation and Environment*, Symp. Soc. Exp. Bio., Cambridge University Press, Cambridge, XIX, 1965, pp. 205-234.
20. J.L. Monteith, Evaporation and surface temperature, *Quarterly Journal of the Royal Meteorological Society* **107** (1981) 1-27.
21. J. E. Nash and J. V. Sutcliffe, River flow forecasting through conceptual models, Part I: A discussion of principles, *J. Hydrol.* **10** (1970) 282-290.
22. Nguyen Ngoc Anh, *The Evaluation of Water Resources in the Eastern Nam Bo, Vietnam*, Project KC12-05, Southern Institute for Water Resources Planning, Ho Chi Minh City 1995, (in Vietnamese).
23. H. L. Penman, Natural evaporation from open water, bare soil and grass, *Proc. Royal Soc. London*, A193, 1948, pp. 120-146.

24. P.J. Sellers, J.A. Berry, G.J. Collatz, C.B. Field, and F.G. Hall, Canopy reflectance, photosynthesis and transpiration, Part III: A re-analysis using improved leaf models and a new canopy integration scheme, *Remots Sens. Environ.* **42** (1992) 187-216.
25. P.J. Sellers, S.O. Los, C.J. Tucker, C.O. Justice, D.A. Dazlich, G.J. Collatz and D.A. Randall, A revised land surface parameterization (SiB2) for atmospheric GCMs, Part II. The generation of global fields of terrestrial biophysical parameters from satellite data, *Journal of Climate* **9** (1996) 706-737.
26. J.B. Stewart, Modelling surface conductance of pine forest, *Agricultural and Forest Meteorology* **43** (1988) 19-35.
27. SWECO International, *Song Bung 4 hydropower project*, TA No. 4625-VIE, Vietnam, 2006.
28. O. Tetens, Uber einige meteorologische, *Begriffe. Z. Geophys.* **6** (1930) 203-204.
29. C.W. Thornthwaite, An approach toward a rational classification of climate, *Geographical Rev.* **38** (1948) 55-94.
30. P.J. Vanderkimpen, Estimation of crop evapotranspiration by means of the Penman-Monteith equation, *Ph.D. thesis*, Utah State University, 1991.
31. D.L. Verseghy, N.A. McFarlance and M. Lazare, CLASS-a Canadian land surface scheme for GCMs, II: Vegetation model and coupled runs, *International Journal of Climatology* **13** (1993) 347-370.
32. C.J. Vorosmarty, C.A. Federer and A.L. Schloss, Potential evaporation functions compared on US watersheds: possible implications for global-scale water balance and terrestrial ecosystem modeling, *J. Hydrol.* **207** (1998) 147-169.
33. M. C. Zhou, H. Ishidaira, H. P. Hapuarachchi, J. Magome, A. S. Keim and K. Takeuchi, Estimating potential evapotranspiration using the Shuttleworth-Wallace model and NOAA-AVHRR NDVI to feed a distributed hydrological modeling over the Mekong River Basin, *J. Hydrol.* **327** (2006) 151-173.

Received March 10, 2008

XÁC ĐỊNH LƯỢNG BỐC THOÁT HƠI TIỀM NĂNG VÀ ẢNH HƯỞNG CỦA NÓ ĐẾN KẾT QUẢ MÔ HÌNH THỦY VĂN

Lượng bốc thoát hơi tiềm năng có thể tính toán trực tiếp bằng phương trình Penman-Monteith, được biết như là phương pháp một bước. Phương pháp này yêu cầu tài liệu về thảm thực vật và các thông số liên quan dựa vào thông tin AVHRR và LDAS sẵn có những năm gần đây. Tiểu vùng Nông Sơn, một phần của lưu vực Vũ Gia-Thu Bồn ở Miền Trung Việt Nam, được chọn cho nghiên cứu này. Mô phỏng quá trình dòng chảy bằng mô hình thuỷ văn (NAM) cho kết quả tốt khi sử dụng giá trị tính toán bốc thoát hơi tiềm năng theo Penman-Monteith.